Available online at www.sciencedirect.com

ScienceDirect

Ceramics International 40 (2014) 4731–4737

CERAMICS INTERNATIONAL

www.elsevier.com/locate/ceramint

Effect of exposure parameters and annealing on the structure and morphological properties of nanopatterned sapphire substrates prepared by solid state reaction

Lin Cui[a,*], Gui-Gen Wang[a], Hua-Yu Zhang[a], Jie-Cai Han[a,b]

[a]Shenzhen Graduate School, Harbin Institute of Technology, Shenzhen 518055, PR China
[b]Center for Composite Materials, Harbin Institute of Technology, Harbin 150080, PR China

Received 21 July 2013; received in revised form 27 July 2013; accepted 5 September 2013
Available online 14 September 2013

Abstract

Nanopatterned sapphire substrates were prepared by solid state reaction of patterned Al films obtained by E-Beam lithography of a PMMA/copolymer bilayer resist and lift-off. The effect of exposure parameters and annealing on the structure and morphological properties of nanopatterned sapphire substrates prepared by solid state reaction were investigated by a scanning electron microscope (SEM), atomic force microscopy (AFM), X-ray diffraction (XRD), and Raman, respectively. The circular Al patterns with diameter/spacing being 500 nm/1000 nm were obtained by optimal exposure diameter/exposure dosage of 400 nm/200 μC/cm^2. Patterned Al films were subsequently subjected to solid state reaction by dual stage annealing due to the melting temperature of Al thin films (660 °C). The hillocks formation on Al films was minimized with an oxidation anneal at 450 °C. Moreover, the little change in the morphology of Al patterns was observed after annealing at 450 °C. The SEM and AFM results show the patterns were retained on sapphire substrates after high temperature annealing at less than 1200 °C. The XRD and Raman results reveal that the composition and orientation of island patterns prepared by solid state reaction for 24 h at 450 °C, and 1 h 1000 °C were the same as that of the sapphire (0001) substrates.

Keywords: Al; Solid state reaction; Annealing; Patterned sapphire substrates; E-Beam lithography

1. Introduction

The high output power GaN-based light-emitting diodes (LEDs) attract much attention because of the various applications in traffic signals, full-color displays, backlight in liquid crystal displays, solid state lighting, and so forth [1]. At present, because of the difficulty of obtaining high-quality and reasonable cost GaN substrates, sapphire is most commonly used as the substrate for LEDs due to its high temperature stability and physical robustness. However, owing to the large lattice mismatch and thermal expansion between the epitaxial GaN film and the underneath sapphire substrate, high threading dislocation densities with the order of 10^9–10^{10} cm^{-2} and deteriorate the electrical and optical properties, therefore, lead to poorer internal quantum efficiency (η_{int}) and reliability [2,3]. In the other hand, the refractive index of nitride films (n=2.5) is higher than that of sapphire substrates (n=1.78) and air (n=1). The critical angle of the escape cone is about 23°, which indicates that about only 4% of the generated light in the active layer can be extracted from the surface and mostly absorbed by the electrode at each reflection and gradually disappears due to total internal reflection, and is then converted to heat [4].

In order to improve the performances of the epitaxial GaN films, the epitaxially lateral overgrowth (ELOG) technique is known to significantly reduce threading dislocations effectively [5–7]. However, ELOG is a time-consuming process and often requires a two step growth procedure and introduces uninterrupted dopants or contaminations. Recently, it has been reported that one can not only reduce the threading dislocation density in GaN films but also enhance the light extraction efficiency by using a patterned sapphire substrate (PSS) [8,9]. In general, PSS are obtained by wet and dry etching. However,

*Corresponding author. Tel.: +86 75526032709.
E-mail addresses: cuilin0512@gmail.com (L. Cui), wanggghit@163.com (G.-G. Wang).

0272-8842/$ - see front matter © 2013 Elsevier Ltd and Techna Group S.r.l. All rights reserved.
http://dx.doi.org/10.1016/j.ceramint.2013.09.016

it is extremely difficult to etch the sapphire substrates by chemical solution at room temperature, because sapphire is chemically inert and highly resistive to acids [10]. Dry etching can provide us an anisotropic profile and a reasonably fast etching rate, but the dry-etched substrates will be inevitably damaged, and the device performance is compromised [11]. Additionally, the dimension of PSS with grooves or other patterns is usually in micron scale range. However, theoretical and experimental studies indicate that a further reduction in defect density is possible if the dimension of the lateral overgrowth patterns is extended to nanoscale range [12,13].

Park and Chan [14] have reported a novel method to fabricate a pristine surface sapphire substrate, via solid state reaction of Al films deposited on sapphire substrates. Beside, patterning is possible at a nanoscale with E-Beam lithography (EBL). This compares to a resolution of ~1 μm for conventional photolithography. No physical mask-plates are needed unlike photolithography, thus eliminating costs and time delays associated with mask production. Patterns can be also optimized and changed very simply using flexible CAD software. In addition, bilayer resist systems are useful for the purpose of an enhanced undercut needed for lifting off thick metal layers. Therefore, to resolve dry and wet etching processes problem, in this study, nanopatterned sapphire substrates (NPSS) were prepared by solid state reaction of patterned Al films fabricated by EBL of a PMMA/copolymer bilayer resist and lift-off. The effect of exposure parameters and annealing on the structure and morphological properties of NPSS prepared by solid state reaction were investigated by a scanning electron microscope (SEM), atomic force microscopy (AFM), X-ray diffraction (XRD), and Raman, respectively.

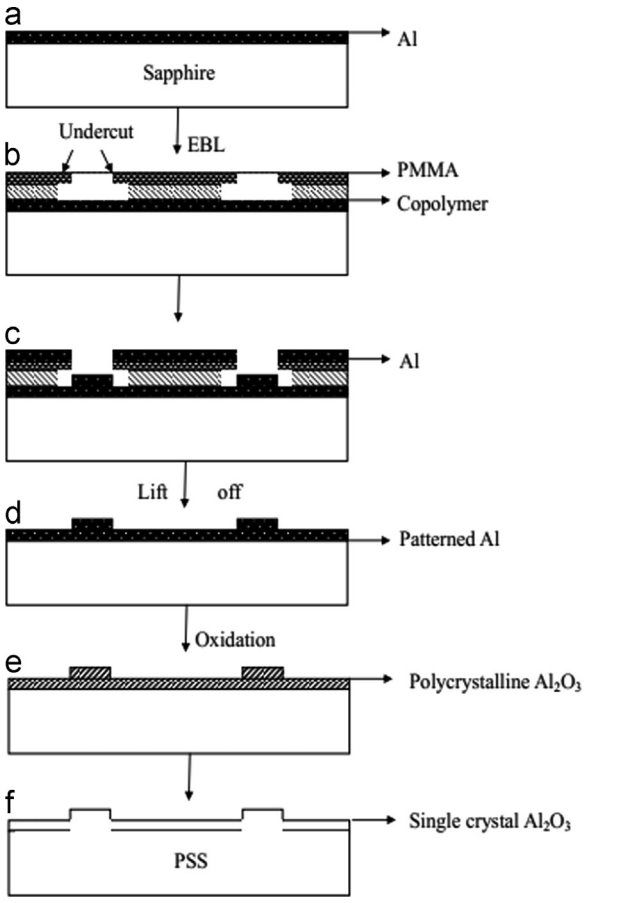

Fig. 1. Schematic diagram showing processing steps in the generation of NPSS by solid state reaction.

2. Experimental

The process of NPSS consisted of the following steps (Fig. 1)(a) To avoid charging effects during subsequent EBL, first, ~10 nm Al films were deposited on sapphire (0001) substrate, (b) EBL of bilayer resist, (c) 130 nm Al films were deposited on patterned EBL resists, (d) patterned Al films were obtained with lift-off process, (e) oxide patterned Al films, and (f) grain growth of patterned polycrystalline alumina films.

High purity Al films were deposited on sapphire (0001) substrates by DC sputtering in a JGP-450a magnetron sputtering system. A prior to deposition, the sapphire substrates were ultrasonically cleaned in acetone for 10 min, alcohol for 10 min, rinsed in deionized water, and then dried in N_2. 99.999% pure Al target of 2-in. diameter was used and plasma of Ar (99.999%) was used for sputtering. The distance between target and substrate was 70 mm. The base pressure was less than 8×10^{-5} Pa. Deposition was carried out at a working pressure of 0.2 Pa after pre-sputtering with Ar for 10 min. When the chamber pressure was stabilized, the DC generator was set to 60 W. The deposition rate utilized was 18 nm/min.

The bilayer resist systems are useful for the purpose of an enhanced undercut (Fig. 1(b)). After cleaning and drying substrate, the 200 nm thick copolymer, methyl MethAcrylate and MethAcrylic Acid [P(MMA–MAA)], was first spin-coated onto ~10 nm thick Al films. At 150 °C, the copolymer was prebaked on a hotplate for 15 min. In the following, a 150 nm thick PMMA was coated immediately to prevent moisture contamination between copolymer and PMMA. The PMMA was then baked at 180 °C for 10 min on a hot plate. E-Beam exposure was carried out with a Raith 150-Turnkey EBL system operating at 10 kV and 0.21 nA beam current. We designed Al patterns with diameter/spacing being 500 nm/1000 nm for exposure diameter and exposure dosage test experiments. The exposure dosages of sample varied from 140 to 260 μC/cm^2. The exposure diameter of sample varied from 300 to 500 nm. After EBL, the exposed PMMA/copolymer was developed by MIBK: IPA (80 s) and then rinsed in IPA (30 s), followed by blow dry by compressed N_2. In the next step, 130 nm Al films were deposited on patterned bilayer resists. The final step of the lift-off process is accomplished by soaking the sample in an acetone bath to wash away the remaining resist and unwanted Al material.

The patterned Al films were subsequently subjected to solid state reaction by dual stage annealing due to the melting temperature of Al thin films (660 °C). The first comprised an oxidation anneal for 24 h, where the annealing temperature was varied in the range of 400–600 °C. The temperature ramp rate was 10 °C/min. This was followed by a high temperature

annealing for 1 h in the range of 800–1200 °C. The temperature ramp rate was 10 °C/min up to 800 °C, and then 5 °C/min thereafter. All solid state reactions were carried out in air in a box furnace with the substrates contained in a high-purity alumina crucible.

In this study, the surface morphology was examined by atomic force microscopy (AFM: Veeco DID3100) and scanning electron microscope (SEM: HITACHI S-4700). The in plane and out of plane orientations were investigated by X-ray diffraction (HRXRD) Philips X' Pert-MRD system with a resolution of 0.005°. The surface microstructure was investigated by Renishaw Micro-Raman system. The excitation was at the 514.5 nm line of an argon ion laser, with 15 mW power, and using a 50 × lens. The backscattering geometry was applied for detection.

3. Results and discussion

For different exposure diameters, different exposure dosages were required to obtain patterned Al films with diameter/spacing being 500 nm/1000 nm, shown in Fig. 2. As shown in Fig. 2, the optimal exposure diameter/exposure dosage was 400 nm/200 μC/cm^2. Top view SEM micrograph of Al patterns with diameter/spacing being 500 nm/1000 nm prepared with optimal exposure parameters is shown in Fig. 3(a). The SEM result reveals that the Al patterns on sapphire substrates had very high accuracy. The top view SEM micrographs of Al patterns exposed with exposure diameter/exposure dosage of 400/140 and 400 nm/260 μC/cm^2 are shown in Fig. 3(b,c). As shown in Fig. 3(b), Al patterns were not observed at exposure dosage of 140 μC/cm^2. Moreover, Al patterns were not accurate at exposure dosage of 260 μC/cm^2 (Fig. 3(c)). This result can be explained by the two reasons: E-Beam exposure dosage was required for thorough thickness penetration of the bilayer resists. For cases where the exposure was insufficient, a continuous layer of resists remained, so that lift-off resulted in the loss of the Al patterns. In the other hand, over exposure is also undesirable, as it degrades the accuracy of the Al patterns.

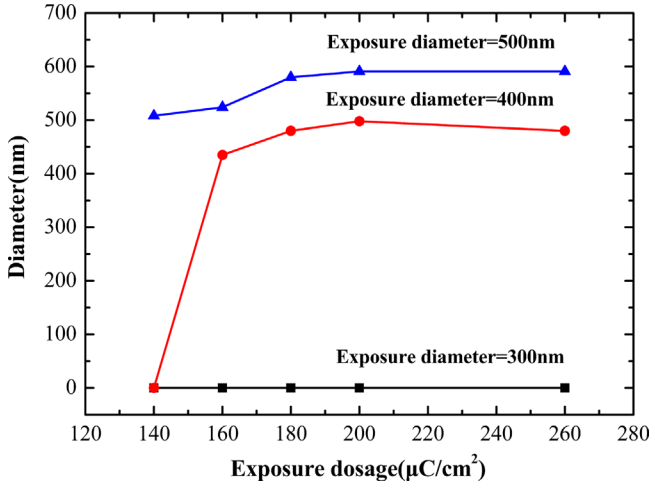

Fig. 2. Al patterns experiment diameter with different exposure diameters and different exposure dosages.

The appearances of 200 nm Al films on sapphire substrates following the oxidation annealing for 24 h in air at 400–600 °C are shown in Fig. 4. As shown in Fig. 4, the surface morphology was generally similar to that in the as-coated state, except for the formation of what appeared to be hillocks on Al films surface. Moreover, the distribution of hillocks was relatively uniform. Our study finds that for the range of conditions studied (400–600 °C), the defect density increased with increasing isothermal annealing temperature. This is consistent with the reports of other hillocking studies, for example, the study of Ericson [15] and Zaborowski [16]. The mismatch in thermal expansion between the Al films and sapphire substrates gives rise to compressive stresses on the Al films [17]. The formation of the hillocks is a stress relaxation mechanism, and several processes for hillock formation have been proposed [18–20]. In this study, it was found the hillocks formation on the surface of Al films was minimized with an oxidation anneal at 450 °C. The morphology of Al patterns following the oxidation annealing for 24 h at 450 °C is shown in Fig. 5(a). As shown in Fig. 5(a), there was little observed change in the morphology of Al patterns following the low temperature oxidation anneal at 450 °C. This result was not unexpected seeing that the oxidation annealing temperature is well below the melting temperature of Al.

More dramatic changes in the pattern morphology were observed following the second high temperature annealing applied to induce grain growth of the sapphire. Fig. 5(b) shows a SEM image of the morphology of the patterned surface after annealing for 24 h at 450 °C, 1 h at 1200 °C. As showed in Fig. 5(b), the smoothing and coalescence of the island features had occurred to such an extent that the pattern was no longer discernible. The phenomenon of surface diffusion driven smoothing of surface features is well established in the literature [21–24] and occurs due to surface energy considerations [25,26]. The kinetics of the smoothing of the circular mesas can be used to derive information on the diffusion mechanism. Therefore, for the successful fabrication of NPSS by solid state reaction, the relative kinetics of smoothing versus grain growth of the underlying sapphire is critical. Fortunately, for high temperature annealing at the lower temperatures used at 1000 and 1100 °C, the patterns were retained. Fig. 5(c) shows a SEM image of the morphology of the patterned surface after high temperature annealing at 1000 °C. Fig. 5(d) shows AFM image of patterned Al films with diameter/spacing being 500 nm/500 nm after dual stage annealing for 24 h at 450 °C, and 1 h at 1000 °C. Using this technique, it can be seen that the upper surfaces of the patterns are not flat. On the contrary, they have an island feature, where the center of the island patterns is higher than the edges. The height of the island patterns following the high temperature annealing of at 1000 °C was ∼140 nm.

The conversion of patterned polycrystalline alumina films to sapphire was characterized by using a HRXRD to investigate the in plane and out of plane orientations. Fig. 6(a) shows the XRD patterns for Al films (200 nm) after annealing for 24 h at 450 °C, and 1 h at 800–1200 °C. As shown in Fig. 6(a), the (0003), (11–20), and (0006) α-Al_2O_3 peaks would exist after

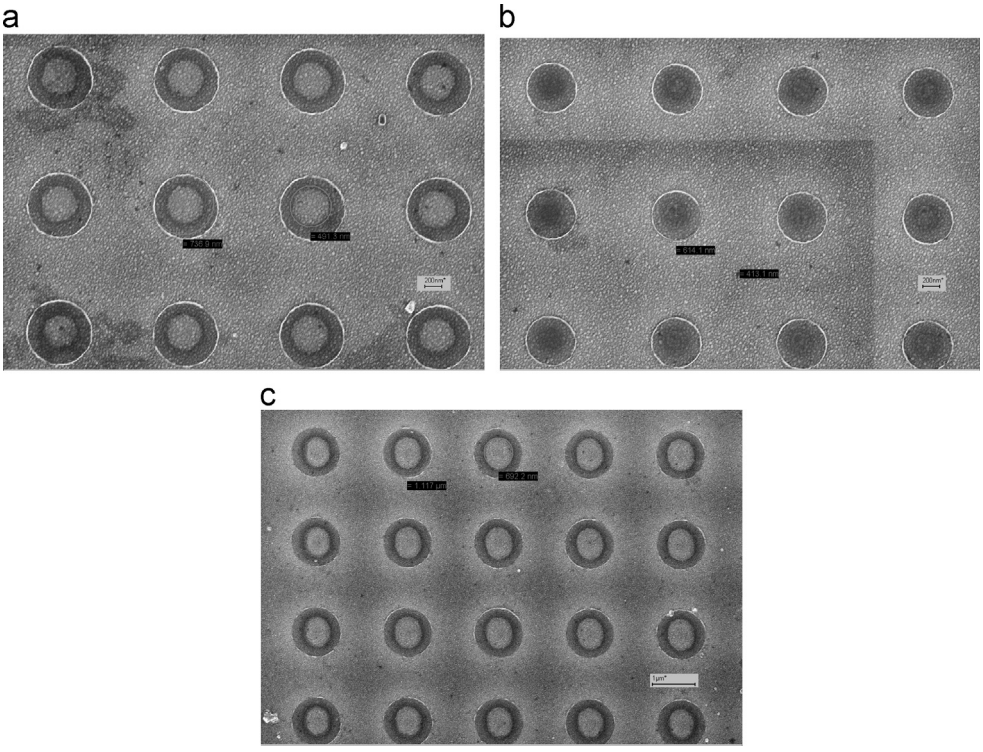

Fig. 3. Top view SEM micrographs of circular patterned Al films with exposure diameter/exposure dosage of 400/200 (a), 400/140 (b), and 400 nm/260 μC/cm^2 (c), respectively.

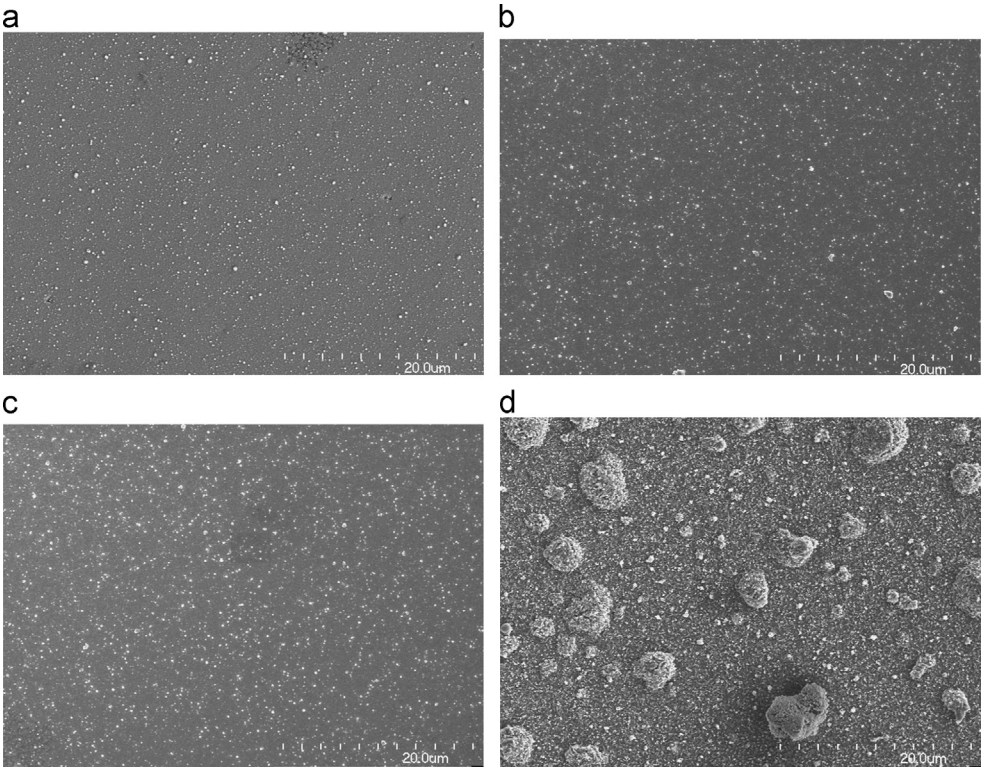

Fig. 4. SEM micrographs depicting surface morphology of Al films (200 nm) on sapphire substrates, subjected to low temperature oxidation anneals for 24 h at 400 °C (a), 450 °C (b), 500 °C (c), and 600 °C (d), respectively.

annealing at 800 °C. The inset shows a detail of (11–20) α-Al_2O_3 peak for Al films after annealing at 800 °C. As shown in Fig. 6(a), Al patterns after annealing at 800 °C were converted to polycrystalline α-Al_2O_3 patterns. However, only *c*-plane peaks would exist after annealing at 900–1200 °C. This implies that the patterns obtained by annealing at 900–1200 °C and sapphire

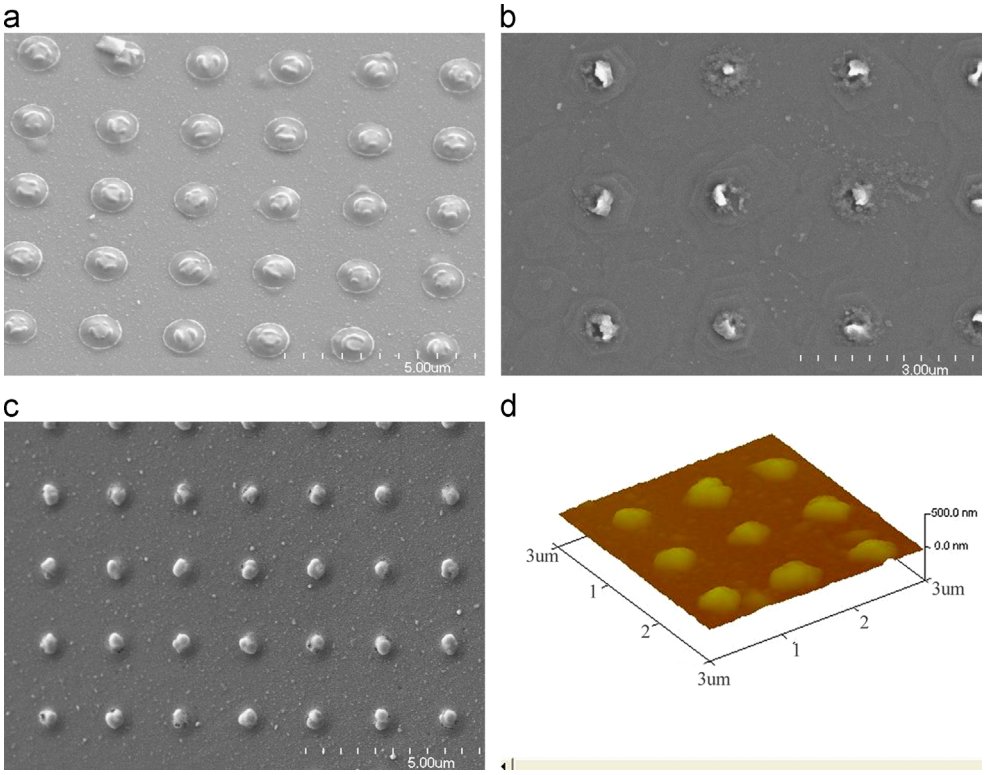

Fig. 5. SEM images of the morphology of the Al patterns on sapphire substrates after annealing for 24 h at 450 °C (a), for 24 h at 450 °C, and 1 h at 1200 °C (b) and 1000 °C (c). AFM images of Al patterns with diameter/spacing being 500 nm/500 nm after annealing for 24 h at 450 °C, and 1 h at 1000 °C (d).

(0001) substrates basal planes were parallel to each other. As shown in Fig. 6(c), six equidistant narrow peaks of Al_2O_3 (11–23) planes are observed in the Φ-scan range of 0–360°, which indicates that the island patterns obtained by annealing at 1000 °C were single crystal α-Al_2O_3. The XRD results reveal that the composition and orientation of island patterns prepared by solid state reaction for 24 h at 450 °C, and 1 h 1000 °C were the same as that of the sapphire (0001) substrates.

Fig. 6(b) shows the Raman spectra for Al films (200 nm) after annealing for 24 h at 450 °C, and 1 h at 800–1200 °C and sapphire (0001) substrates. As shown in Fig. 6(b), seven Raman modes with peaks at ~375, 413, 427, 440, 573, 642, 748 cm^{-1} are observed in sapphire (0001) substrates and Al films (200 nm) after annealing at 900–1200 °C, which is in agreement with the spectrum of natural crystal [27]. The Raman bands with peaks at ~375, 413, 427, 440, 573, 642, 748 cm^{-1} have been assigned to E_g (external), A_{1g} (internal), E_g (external), E_g (external), E_g (internal), A_{1g} (internal), E_g (external) modes, respectively. However, Raman mode with peak at ~375 cm^{-1} is not observed in Al films (200 nm) after annealing at 800 °C. This might be due to the fact that vibrational spectrum of the crystal is modified even by slight changes in the crystal structure [28]. Moreover, the reflected Raman scatter signal obviously increases with the annealing temperature increasing from 900 to 1200 °C. The stronger Raman signal and the more complete the Raman spectrum characteristic line, the higher the quality of specimen surface. The Raman results are consistent with the results of XRD. Thus, it is believed that the above process has potential for the fabrication of NPSS for the high output power GaN-based light-emitting diodes.

4. Conclusion

In this study, NPSS were prepared by solid state reaction of patterned Al films obtained by EBL of a PMMA/copolymer bilayer resist and lift-off. The effect of exposure parameters and annealing on the structure and morphological properties of NPSS prepared by solid state reaction were investigated by a scanning electron microscope (SEM), atomic force microscopy (AFM), X-ray diffraction (XRD), and Raman, respectively. The circular Al patterns with diameter/spacing being 500 nm/1000 nm were obtained by optimal exposure diameter/exposure dosage of 400 nm/200 μC/cm^2. Patterned Al films were subsequently subjected to solid state reaction by dual stage annealing due to the melting temperature of Al thin films (660 °C). The hillocks formation on Al films was minimized with an oxidation anneal at 450 °C. Moreover, the little change in the morphology of Al patterns was observed after annealing at 450 °C. The SEM and AFM results show the patterns were retained on sapphire substrates after high temperature annealing at less than 1200 °C. The XRD and Raman results reveal that the composition and orientation of island patterns prepared on sapphire (0001) substrates by solid state reaction for 24 h at 450 °C, and 1 h 1000 °C were the same as that of the sapphire (0001) substrates. It is believed that the above process has potential for the fabrication of NPSS for the high output power GaN-based light-emitting diodes.

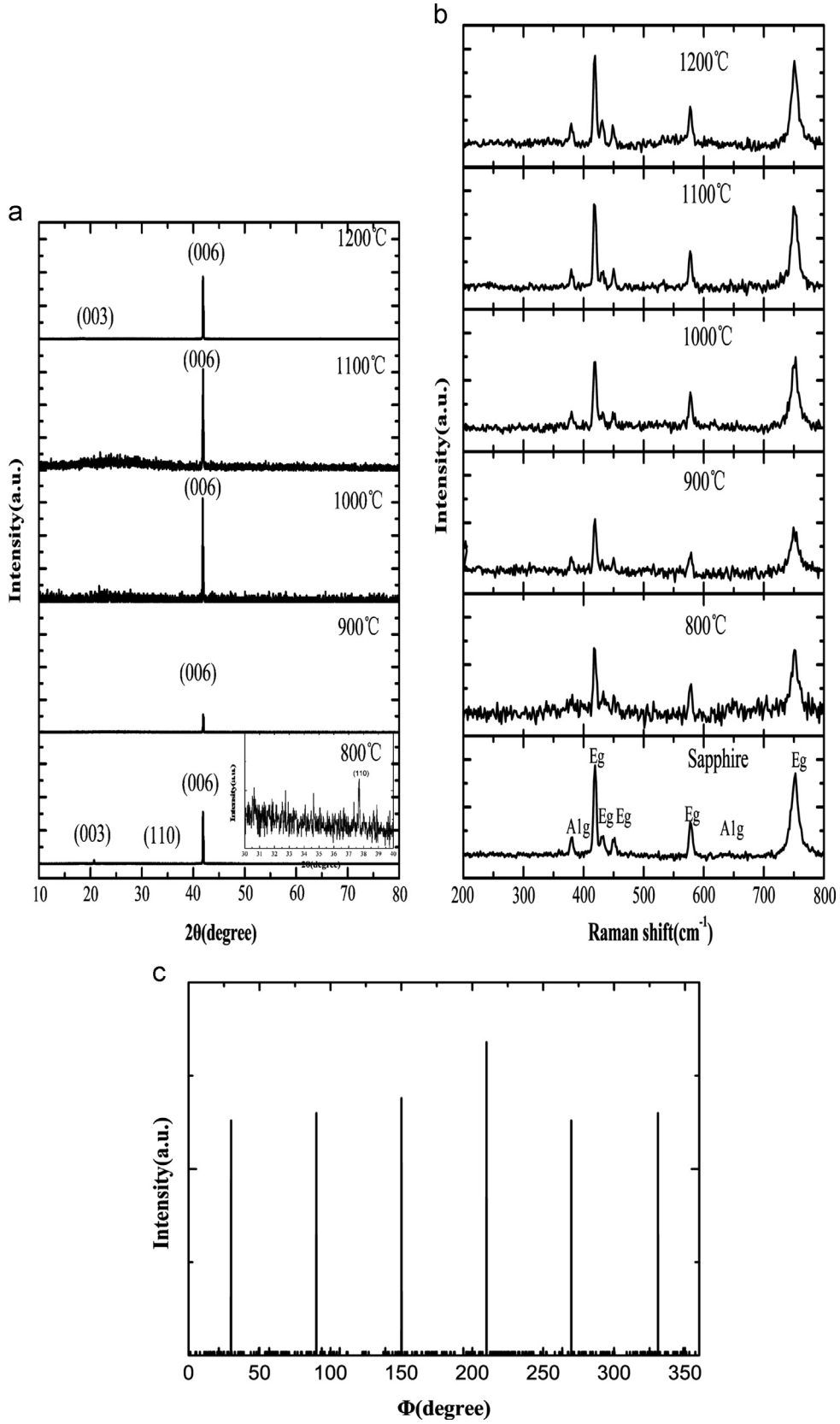

Fig. 6. X-ray diffraction patterns (a) and Raman spectra (b) for Al films (200 nm) on sapphire substrates after annealing for 24 h at 450 °C, and 1 h at 800–1200 °C. (11–23) Φ-scan of Al films (200 nm) on sapphire substrates after annealing for 24 h at 450 °C, and 1 h at 1000 °C (c).

Acknowledgments

This project was supported by the National Natural Science Foundation of China (Grant No. 50902028), the Natural Science Foundation of Guangdong Province (Grant No. 9451805707003351), the Weapon & Equipment Pre-research Foundation of General Armament Department (Grant No. 9140A12050213HT01175), the Basic Research Plan Program of Shenzhen City in 2012 (Grant No. JCYJ20120613134210982), and the Natural Scientific Research Innovation Foundation in Harbin Institute of Technology (Grant No. HIT.NSFIR.2011123).

References

[1] E.F. Schubert, Light Emitting Diodes, 2003 Cambridge University Press, Cambridge, UK (2003), chap. 19-20.
[2] A. Usui, H. Sunakawa, A. Sakai, A.A. Yamaguchi, Thick GaN epitaxial growth with low dislocation density by hydride vapor phase epitaxy, Japanese Journal of Applied Physics 36 (1997) L899–L902.
[3] M. Iwaya, T. Takeuchi, S. Yamaguchi, C. Wetzel, H. Amano, I. Akasaki, Reduction of etch pit density in organometallic vapor phase epitaxy-grown GaN on sapphire by insertion of a low-temperature-deposited buffer layer between high-temperature-grown GaN, Japanese Journal of Applied Physics 37 (1998) L316–L318.
[4] C. Huh, K.S. Lee, E.J. Kang, S.J. Park, Improved lightoutput and electrical performance of InGaN-based light-emitting diode by micro-roughening of the pGaN surface, Journal of Applied Physics 93 (2003) 9383–9385.
[5] K. Tadatomo, H. Okagawa, Y. Ohuchi, T. Tsunekawa, Y. Imada, M. Kato, T. Taguchi., High output power InGaN ultraviolet light-emitting diodes fabricated on patterned substrates using metal organic vapor phase epitaxy, Japanese Journal of Applied Physics 40 (2001) L583–L585.
[6] M. Yamada, T. Mitani, Y. Narukawa, S. Shioji, I. Niki, S. Sonobe, K. Deguchi, M. Sano, T. Mukai, InGaN-based near-ultraviolet and blue-light-emitting diodes with high external quantum efficiency using a patterned Sapphire substrate and a mesh electrode, Japanese Journal of Applied Physics 41 (2002) L1431–L1433.
[7] Z.H. Feng, K.M. Lau, Enhanced luminescence from GaN-based blue LEDs grown on grooved sapphire substrates, IEEE Photonics Technology Letters 17 (2005) 1812–1814.
[8] Joonhee Lee, Dong-Ho Kim, Jaehoon Kim, Heonsu Jeon, GaN-based light-emitting diodes directly grown on sapphire substrate with holographically generated two-dimensional photonic crystal patterns, Current Applied Physics. 9 (2009) 633–635.
[9] C.B. Soh, K.H. Dai, W. Liu, S.J. Chua, R.J.N. Tan, A.M. Yong, Jack Eng, Enhancement in light extraction efficiency from GaN based LEDs with nanopores ITO p-contact grown on patterned sapphire substrate, Physica Status Solidi B 247 (2010) 1757–1760.
[10] S. Nakamura, T. Mukai, M. Senoh, Candela-class high-brightness InGaN/AlGaN double-heterostructure blue-light-emitting diodes, Applied Physics Letters 64 (1994) 1687–1689.
[11] Fawang Yan, Haiyong Gao, Yang Zhang, Jinmin Li, Yiping Zeng, Guohong Wang, Fuhua Yang, High-efficiency GaN-based blue LEDs grown on nano-patterned sapphire substrates for solid-state lighting, Proceedings of SPIE 6841 (2007) (684103-01-684103-02).
[12] S.D. Hersee, D. Zubia, X. Sun, R. Bommena, M. Fairchild, S. Zhang, D. Burckel, A. Frauenglass, S.R.J. Brueck, Nanoheteroepitaxy for the integration of highly mismatched semiconductor materials, IEEE Journal of Quantum Electronics 38 (2002) 1017–1028.
[13] Yung-Chun Lee, Yi-Ta Hsieh, Chen-Yu Chiu, Direct metal contact printing lithography for patterning sapphire substrate and enhancing light extraction efficiency of light-emitting diodes, Journal of Micromechanics and Microengineering 21 (2011) 015001-01–015001-03.
[14] H. Park, H.M. Chan., A novel process for the generation of pristine sapphire surfaces, Thin Solid Films 422 (2002) 135–140.
[15] F. Ericson, N. Kristensen, J. Schweitz., A transmission electron microscopy study of hillocks in thin aluminum films, Journal of Vacuum Science and Technology B (1991) 958–963.
[16] M. Zaborowski, P. Dumania, Kinetics of hillock growth in Al and Al-alloys, Microelectronic Engineering 50 (2000) 301–309.
[17] G. Dehm, B.J. Inkson, T. Wagner, Growth and microstructural stability of epitaxial Al films on (0001)-Al_2O_3 substrates, Acta Materialia 50 (2002) 5021–5032.
[18] D. Kim, B. Heiland, W.D. Nix, E. Arzt, M.D. Deal, J.D. Plummer, Microstructure of thermal hillocks on blanket Al thin films, Thin Solid Films 371 (2000) 278–282.
[19] D. Kim, W.D. Nix, R.P. Vinci, M.D. Deal, J.D. Plummer, A study of the effect of grain boundary migration on hillock formation in Al thin films, Journal of Applied Physics 90 (2001) 781–788.
[20] C.Y. Chang, R.W. Vook, The effect of surface aluminum oxide films on thermally induced hillock formation, Thin Solid Films 228 (1993) 205–209.
[21] T. Maruyama, W. Komatsu, Surface diffusion of single-crystal Al_2O_3 by scratch-smoothing method, Journal of the American Ceramic Society 58 (1975) 338–339.
[22] S.J. Bennison, M.P. Harmer, Effect of MgO solute on surface diffusion in sapphire and the role of MgO in the sintering of Al_2O_3, Journal of the American Ceramic Society 73 (1990) 833–837.
[23] A.M. Glaeser, Ceramic Interfaces. Properties and Applications, Inst. Mater, London, UK (1998), p. 241.
[24] H.P. Bonzel, Surface morphologies. Transient and equilibrium shapes, Interface Science 9 (2001) 21–34.
[25] W.W. Mullins, Flattening of a nearly planar solid surface due to capillarity, Journal of Applied Physics 30 (1959) 77–83.
[26] H.P. Bonzel, W.W. Mullins, Smoothing of perturbed vicinal surfaces, Surface Science 350 (1996) 285–300.
[27] C.J. Karr, Infrared and Raman Spectroscopy of Lunar and Terrestrial Mineral, Academic Press, New York, 1975.
[28] M. Kadleikova, J. Breza, M. Vesely, Microelectronics Journal 32 (2001) 955–958.